

Cortico–basal ganglia circuit mechanism for a decision threshold in reaction time tasks

Chung-Chuan Lo & Xiao-Jing Wang

Growing evidence from primate neurophysiology and modeling indicates that in reaction time tasks, a perceptual choice is made when the firing rate of a selective cortical neural population reaches a threshold. This raises two questions: what is the neural substrate of the threshold and how can it be adaptively tuned according to behavioral demands? Using a biophysically based network model of spiking neurons, we show that local dynamics in the superior colliculus gives rise to an all-or-none burst response that signals threshold crossing in upstream cortical neurons. Furthermore, the threshold level depends only weakly on the efficacy of the cortico-collicular pathway. In contrast, the threshold and the rate of reward harvest are sensitive to, and hence can be optimally tuned by, the strength of cortico-striatal synapses, which are known to be modifiable by dopamine-dependent plasticity. Our model provides a framework to describe the main computational steps in a reaction time task and suggests that separate brain pathways are critical to the detection and adjustment of a decision threshold.

Decision making proceeds from deliberation to choice selection. Deliberation is a gradual process, usually taking a longer time when a decision is harder or when more choice options must be considered, whereas choosing one of the possible alternatives is categorical, often in the form of an overt action. For decades, psychologists have used reaction time tasks to probe the process of accumulation of information in perceptual decisions. Extensive behavioral analyses have led to mathematical models in which sensory information is integrated stochastically over time, resulting in a random walk of an abstract variable toward a preset decision threshold. A decision is made when the random walker reaches the threshold^{1–4}.

Recently, neurophysiological studies on nonhuman primates have discovered single-neuron activities correlated with time integration of sensory information during perceptual decisions. In a reaction time version of a random-dot motion direction discrimination task (Fig. 1a,b)⁵, neurons in the lateral intraparietal (LIP) area were found to be correlated with the monkey's decision process. Specifically, when averaged over trials in which the monkey's chosen motion direction was toward the response field of a recorded LIP cell, the cell's firing activity showed a ramping time course during stimulus presentation, and the ramping slope was larger with a stronger motion strength (higher quality of sensory information), defined by the fraction of dots moving coherently in the same direction⁶. Furthermore, the decision choice (as signaled by a saccade) was made when the average firing rate of a selective population of parietal neurons reached a threshold, which was independent of the coherence level and the response time⁶. Similar decision-correlated neural activity has also been reported in prefrontal cortex during the same visual motion discrimination task⁷ and in the frontal eye field during a visual countermanding task^{8,9}. These observations indicate that the activity of cortical neurons resembles the

behavior predicted by models in psychology^{7,10–12}. A biophysically based neural network model^{13,14} offers a similar but modified picture, in which neural groups selective for opposite directions of motion compete with each other through local recurrent synaptic inhibition. Moreover, the model proposes a candidate cellular mechanism (slow reverberatory network dynamics mediated by NMDA receptors) for the continuous accumulation of the sensory information (visual stimulus in the random-dot task) over time.

Both empirical observations and theoretical analyses suggest that ramping activity in cortical networks during stimulus presentation only indicates the likelihood of a decision choice^{10,11}. The actual decision relies on downstream neurons' ability to detect the event of threshold crossing and to pass this information to motor systems. It is also suggested that the threshold can be tuned to optimize the trade-off between speed and accuracy^{11,15}. We thus ask the following questions: (i) what is the neural substrate of a decision threshold, (ii) how is the threshold-crossing event read out, and (iii) can the threshold be tuned by biologically plausible mechanisms to optimize a decision-making process^{11,15,16}? In this paper, we address these questions by using biophysically based circuit modeling. We considered a large-scale network of interconnected cortex, superior colliculus and basal ganglia. The idea is that threshold crossing of ramping cortical neural activity may be detected by neurons in a downstream motor command center, which is presumably the superior colliculus in the case of saccadic eye movements¹⁷. Indeed, burst neurons in the intermediate layer of the superior colliculus receive inputs from many cortical areas, including the parietal cortex, and project to midbrain neurons responsible for the generation of saccadic eye movements^{17–20}. These burst neurons are typically silent when the eyes are fixated, but fire immediately before a saccade at a rate of around 200–300 Hz for less than 100 ms. Based on

Volen Center for Complex Systems, Brandeis University, Waltham, Massachusetts 02254, USA. Correspondence should be addressed to X.-J.W. (xjwang@brandeis.edu).

Received 24 January; accepted 22 May; published online 11 June 2006; doi:10.1038/nn1722

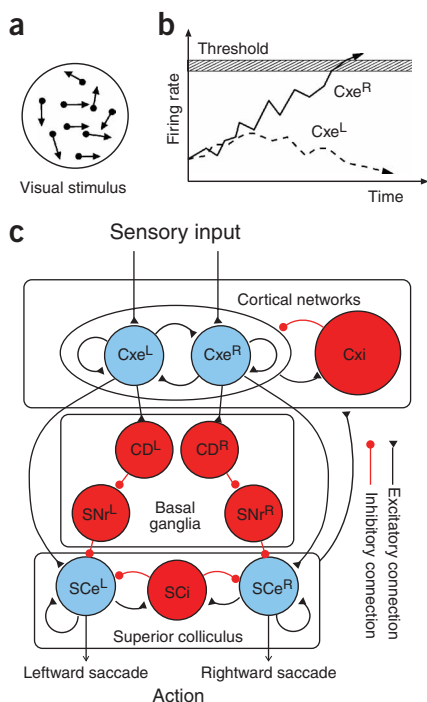


Figure 1 A large-scale brain network model for the reaction time version of a random-dot task. **(a)** In the task, a subject is shown a display of randomly moving dots. The subject is required to hold his or her gaze at a fixed point on the screen while figuring out the net motion direction of the dots. As soon as a decision is reached, the subject indicates the direction of dot motion by a saccadic eye movement. **(b)** A schematic picture showing that firing rates of two cortical populations (Cxe^R and Cxe^L) slowly change in response to sensory inputs (random-dot motion). A saccade is made whenever one of the population firing rates reaches the threshold. **(c)** Schematic model architecture. Neural pools in the cortical network integrate sensory information and also compete against each other. They project to both the superior colliculus and the caudate nucleus in the basal ganglia. Blue, populations of excitatory neurons; red, populations of inhibitory neurons. Each population is simulated by noisy spiking leaky integrate-and-fire neurons.

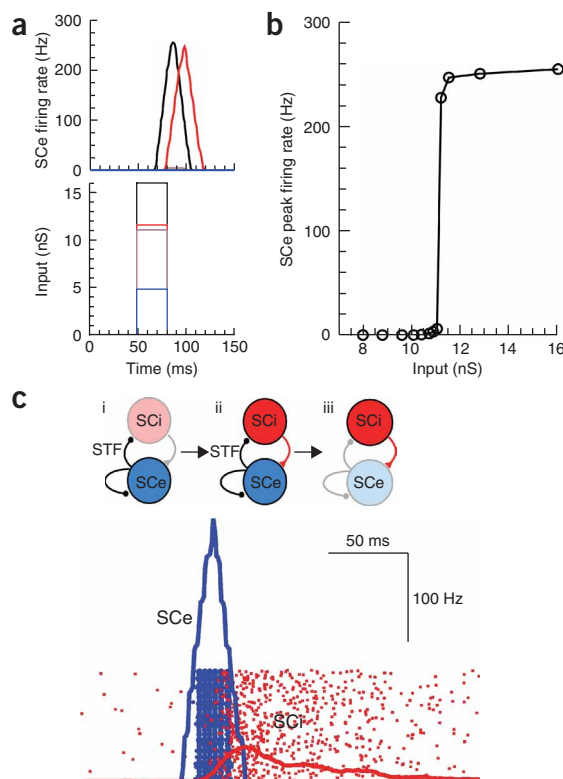
decision process through the striatum^{31–33}. Based on these observations, we incorporated the cortico-collicular and cortico-basal ganglia pathways into our model. By using a phase plane analysis, we reveal a parallel circuit mechanism, in which the two pathways have distinct roles in the detection and adaptive tuning of a decision threshold.

RESULTS

Our model was designed for the reaction time version of the random-dot direction-discrimination task⁶. The model consists of three brain areas (**Fig. 1**): the cortex (Cx), the superior colliculus (SC) and the basal ganglia (BG). Each of the three networks contains competing neural populations selective for left or right motion directions (denoted by superscript L or R, respectively), and this selectivity is preserved along the processing stages (**Fig. 1c**; details of model in Methods). The cortical neurons slowly accumulate information about the stimulus over time (**Fig. 1b**). The neural population receiving a stronger input has a higher probability of ramping up its firing rate and winning the competition; this process is stochastic because of irregular neuronal

in vitro electrophysiological data^{17,21–24}, we built a recurrent network model for the superior colliculus burst cells, and we tested the hypothesis that these burst cells are suitable for reading out threshold crossing in upstream neurons. Furthermore, the superior colliculus is known to be under the control of the basal ganglia, which have a critical role in voluntary motor behavior in general^{25–28}. Neurons in substantia nigra pars reticulata (SNr), an output structure of the basal ganglia, send GABAergic projections to principal cells in the superior colliculus and exhibit baseline activity as high as 50–100 Hz, providing a ‘default’ tonic inhibition to the superior colliculus. This inhibition is released when the SNr receives increased inhibitory inputs from caudate nucleus (CD, part of the striatum), which is driven by excitatory inputs from many cortical areas including the LIP and frontal eye field^{25,29}. Thus, the cortico-basal ganglia pathway has a modulatory role in the generation of saccadic eye movements. In addition, the striatum is the recipient of prominent projections from midbrain dopamine neurons^{25,30}, suggesting that reward-related signals may modulate the

Figure 2 Threshold detection by burst discharge in the superior colliculus network. **(a)** SCe neurons display a strong burst of spikes (top) only when the input exceeds a certain threshold level (bottom). Each input and its corresponding SCe response are plotted with the same color. Note that a larger input above the threshold shortens the response latency but does not alter the shape of the stereotypical burst. **(b)** The SCe neuronal response (peak spiking rate) is a step function of the input amplitude, indicating a sharply defined threshold. The curve is drawn from the data shown in **a**. **(c)** Interaction between excitatory (SCe) and inhibitory (SCi) neurons underlies SCe burst generation. Schematic of sequential events (top): SCe neurons are first activated by the input and develop a strong response due to recurrent excitation (i); then SCe neurons activate SCi neurons slowly, through synapses endowed with short-term facilitation, until SCi neurons are excited (ii); finally, activated SCi neurons quickly inhibit SCe (iii) and the system goes back to the initial state. Bottom, population firing rates (blue and red curves), overlapped with rasters (blue and red dots, each row of dots represent the spiking activity of a neuron) in a simulated trial, demonstrate that SCe neurons develop a strong but brief burst of activity as a result of the interaction between SCe and SCi.



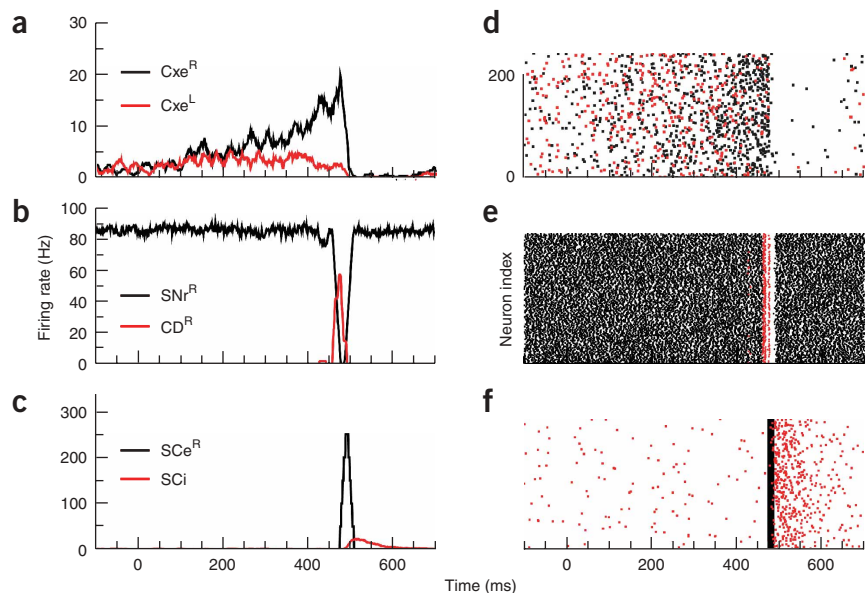
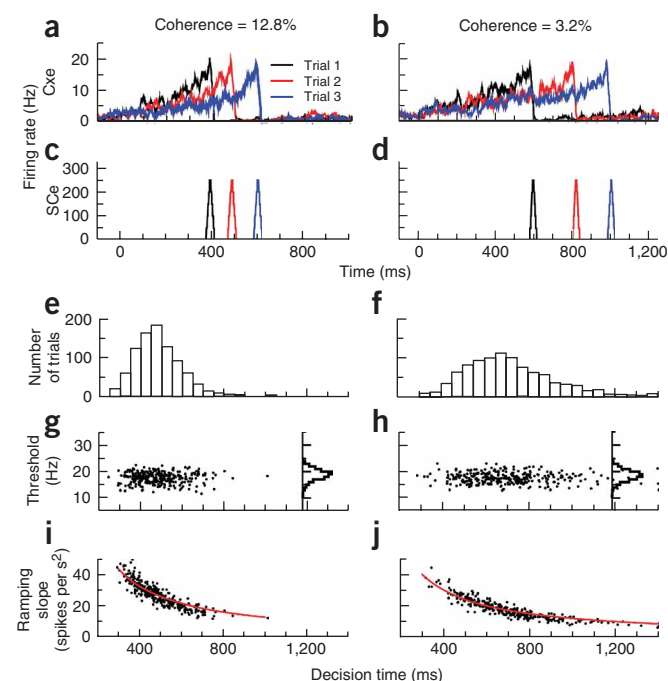


Figure 3 Reaction time simulation by the full network model, in a single trial with motion coherence of 12.8%. (a–c) Population firing rates of Cxe, SNr and CD, and SCe and SCi demonstrate that a SCe burst is triggered when the firing rate of one of the Cxe populations excites the corresponding CD, which in turn inhibits the SNr and releases its inhibition on SCe. (d–f) Corresponding rasters of population firing rates in a–c. $t = 0$ corresponds to stimulus onset.

spiking dynamics. We now examine how such cortical signals are used by downstream systems.

Burst response in the superior colliculus network

We first consider the behavior of an isolated SC network. During saccadic behavior, cells in the superior colliculus exhibit a variety of firing patterns and have been classified into burst cells, buildup cells



Gating mechanism in the basal ganglia network

We have shown that the all-or-none response of the SC to cortical inputs can detect a threshold crossing event in the input. We now consider how this mechanism serves decision making in the full Cx-BG-SC network model. We first demonstrate a single-trial simulation of the full network model (Fig. 3). At the beginning of the trial, firing rates of Cxe populations start to increase in response to their sensory inputs. In the meantime, due to inhibition from the SNr, SCe neurons remain silent even though the inputs from the Cxe exceed the firing threshold of SCe neurons (6.7 Hz in the model in the absence of inhibition from the SNr). When the firing rate of Cxe^R is large enough, it activates the corresponding CD^R, which in turn shuts down SNr^R and releases SCe^R from inhibition. When SCe^R fires a strong burst, it triggers a motor response (signaling the choice), and at the same time sends a ‘corollary discharge’ back to both excitatory and inhibitory neurons in the Cx. The activated inhibitory neurons ultimately reset the Cx network to rest.

Figure 4 Invariance of the threshold across trials, regardless of decision times and coherence levels. (a–d) Three trials are shown for each of 12.8% and 3.2% coherence levels. Firing rate traces of a Cxe population (a,b) indicate that Cxe always triggers a burst in SCe (c,d) when the firing rate of Cxe reaches about the same level. $t = 0$ corresponds to stimulus onset. (e,f) Distributions of decision time. (g,h) Threshold level (defined as the Cxe firing rate that triggers an SCe burst) as a function of the decision time (each data point corresponds to an individual trial). Insets in g and h, distribution of threshold. The threshold is independent of the decision time, even though the latter varies considerably with the motion coherence as shown in e and f. (i,j) The ramping slope of Cxe firing rate is inversely related to decision time (each data point corresponds to an individual trial). Ramping slope is calculated by running a linear regression on Cxe firing rate for the time epoch starting from when the firing rate hits 5 Hz for the first time until the saccade onset. The red curve is $1,300/(\text{decision time})$ in i and $12,000/(\text{decision time})$ in j.

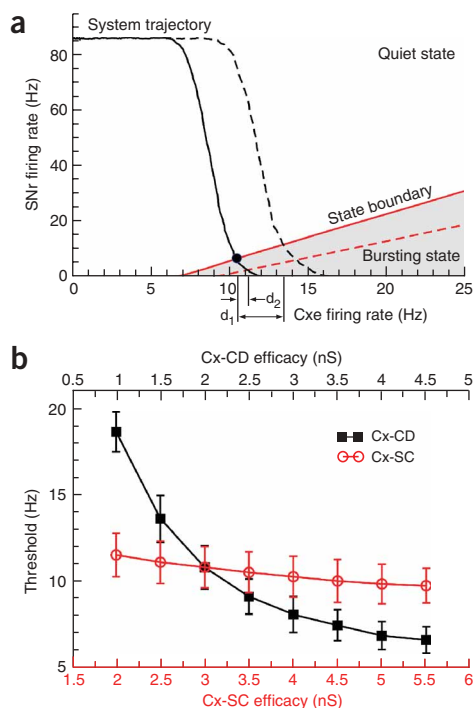


Figure 5 Roles of cortico-collicular (Cx-SC) and cortico-striatal (Cx-CD) pathways in the determination of the decision threshold. **(a)** Behavior of SCell neurons on a phase plane in which SNr and Cxe firing rates are plotted against each other. The two SCell states, quiet state (white region) and burst firing state (gray region), are separated by the state boundary (red curve). The decision threshold (black circle) is determined by the intersection of the state boundary and the dynamical trajectory (black curve) that the network system follows over time in response to sensory inputs. The position of the state boundary can be shifted by changing the efficacy of Cx-SC synapses (3.5 nS for the red solid curve and 2.5 nS for the red dashed curve), and the position of the dynamical trajectory can be shifted by changing the Cx-CD synaptic efficacy (2.1 nS for the black solid curve and 1.5 nS for the black dashed curve). As shown in the figure, the decision threshold is efficiently modified by synaptic modification of the Cx-CD pathway (d_1) but not by that of the Cx-SC pathway (d_2). **(b)** Quantification of the finding in **a**, which shows the dependence of the decision threshold on the efficacy of Cx-CD and Cx-SC synapses. Each point is the average over 100 trials. Error bars indicate s.d.

For a given coherence level, the decision time, defined by the time it takes from the beginning of the stimulus to the burst onset, varies markedly across trials (Fig. 4a–d), and the trial-averaged decision time increases with decreasing coherence (Fig. 4e,f). Yet, the decision threshold, defined by the Cxe firing rate needed to activate the SC, remains roughly constant across trials and is independent of the coherence level (Fig. 4g,h). For coherence = 3.2% and 12.8%, the estimated mean Cxe firing threshold is indistinguishable (17.9 Hz versus 17.6 Hz) and the s.d. is the same (2 Hz); hence the variability of decision times is not attributable to that of the decision threshold. Furthermore, on a trial-by-trial basis, the ramping slope of Cxe firing activity is inversely correlated with the decision time (Fig. 4i,j). Note that a fixed threshold implies that the product of the ramping slope and decision time is roughly constant across trials, which is supported by the observed inverse relationship between the two (Fig. 4i,j). Hence, a reliable threshold detection mechanism is realized in our model.

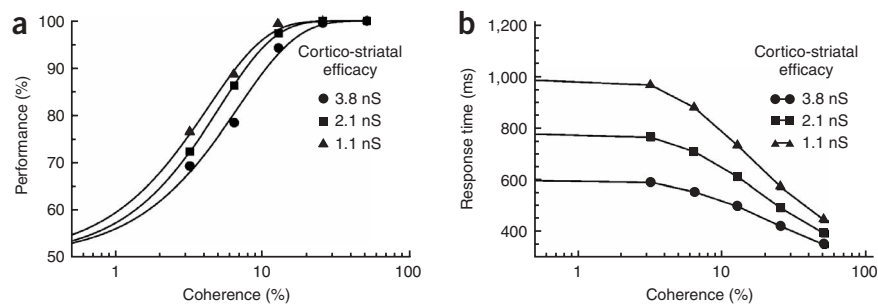
Modulation of the decision threshold

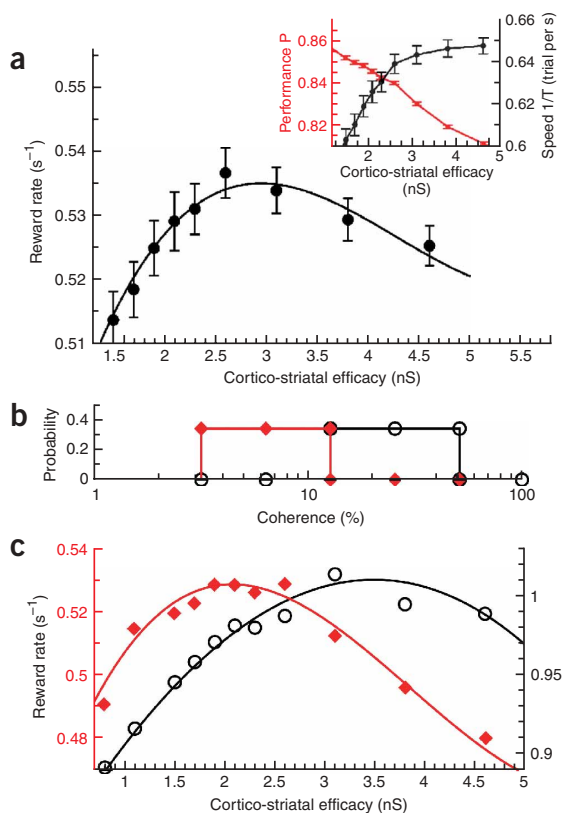
To dissect the differential contributions of the Cx-SC and Cx-CD pathways to the threshold mechanism, we found it instructive to consider the model's dynamics in a two-dimensional 'phase plane' in which SNr firing rate is plotted against Cxe firing rate (Fig. 5a). SCell has

two states (quiet and bursting), which are determined by the firing rates of the SNr and the Cxe. The model system follows a trajectory (black solid curve in Fig. 5a). At stimulus onset, the system starts from the left upper corner of the phase plane where the Cxe has a low firing rate and the SNr shows tonic activity around 80 Hz. As time proceeds, the Cxe firing rate ramps up until it is large enough to activate the CD and shut down the SNr, indicated by the abrupt drop in the trajectory in the middle of the phase plane. SCell starts to fire when the trajectory hits the boundary (red solid curve). Therefore, the decision threshold is determined by the intersection of the system trajectory and the state boundary. In this example the threshold is around 10.5 Hz.

The phase plane indicates that the decision threshold can be changed by shifting either the system trajectory or the state boundary. We found that the state boundary can be shifted by varying the efficacy of Cx-SC synapses. However, the shift in the state boundary results in a very small change in the threshold (shift from the red solid curve to the red dashed curve in Fig. 5a). On the other hand, the system trajectory can be shifted by changing the efficacy of Cx-CD synapses. The shift in the system trajectory produces a drastic change in the decision threshold (shift from the black solid curve to the black dashed curve in Fig. 5a). We verified this observation by plotting the decision threshold as functions of Cx-CD and Cx-SC synaptic efficacies (Fig. 5b): the range of threshold values is substantially larger when we vary the efficacy of the Cx-CD pathway (black curve), as compared with that of the Cx-SC pathway (red curve). Note that this conclusion assumes that when the SNr activity starts to decrease, the change is abrupt. Indeed, imagine that this drop was exactly a vertical line, then no shift of threshold could possibly be induced by changing the state boundary. On the other hand, if the SNr trajectory was very smooth—that is, showing a slow and gradual time course—then varying the Cx-SC synaptic strength would be able to shift the threshold more efficiently. However, this possibility does not seem to be consistent with the

Figure 6 Dependence of psychometric and chronometric functions on the Cx-CD efficacy. **(a,b)** Performance (percentage of correct choices) and response time are plotted as functions of the motion coherence c' . When Cx-CD efficacy increases (producing a lower decision threshold), the performance decreases, but the response speed (inverse of response time) increases, resulting in a trade-off between speed and accuracy (see Fig. 7). Data points in **a** are fitted with the Weibull function $p = 100(1 - 0.5 \times \exp(-(c'/\beta)^\alpha))$, where β and α are constants estimated for each curve.





physiological observation that SNr cells typically display a precipitous decrease of firing rate immediately before a saccade^{34,35}. Therefore, our phase plane analysis of a physiologically constrained model suggests that, although the threshold crossing (and hence response timing) is detected through the Cx-SC pathway, the threshold value itself may be more easily adjusted through the Cx-CD pathway.

Speed-accuracy trade-off and decision optimization

We next investigated how the cortico-striatal (Cx-CD) synaptic efficacy affects the performance and average response time. For a given Cx-CD synaptic efficacy, the network decision behavior is quantified by the psychometric and chronometric functions (percentage of correct choices and mean response time as a function of the coherence level) (Fig. 6). When the Cx-CD synaptic efficacy is decreased, the threshold increases and both the performance (percentage of correct choices) and the average response time increase. These changes affect the overall reward rate R , which can be calculated as the number of correct (rewarded) trials per unit time, or $R = P/T$ where P is the average percentage of correct choices and T is the average trial duration (Methods).

We found that there is an optimal value of the Cx-CD efficacy for which the reward rate R is maximal (Fig. 7a). The reward rate drops when Cx-CD efficacy increases or decreases from this optimal value, suggesting that the maximum reward rate can be achieved by tuning the Cx-CD efficacy. This can be intuitively explained by a speed-accuracy trade-off¹¹: a very low threshold reduces the decision times but yields more errors, whereas a sufficiently high threshold improves performance yet prolongs decision times. Neither is ideal for maximizing the reward amount per unit time. To further test this interpretation, we manipulated the degree of task difficulty. Instead of a uniform distribution of coherence levels, we considered an easier or harder task by using only high or low coherence levels (black versus red, Fig. 7b).

Figure 7 Optimization of decision-making process. (a) A maximum reward rate is achieved by tuning the Cx-CD efficacy. Each point is calculated from a block of trials with a uniform distribution of coherence levels. The reward rate R is defined as $R = P/T$, where P is the average performance and T is the average trial time duration (see inset for P and $1/T$). Error bars indicate s.e.m. The optimal Cx-CD efficacy that maximizes the reward rate occurs at around 2.6 nS. The maximum reward rate equals 0.537 reward per second, with an average performance of 84.0% and an average response time of 585 ms (excluding the intertrial intervals and penalty times). (b,c) The optimal efficacy depends on task conditions. If we alter the degree of task difficulty by using different probability distributions of coherence levels (as shown in b), the optimal synaptic efficacy shifts toward a larger value (3.1 nS) in the easy task (black) and toward a smaller value (2.0 nS) in the hard task (red) (as shown in c). Correspondingly, the optimal decision threshold is lower for an easy task and higher for a difficult task. To visualize the relationship between the reward rate and cortico-striatal efficacy, we fitted data in a and c with cubic polynomials (solid curves).

As expected, the Cx-CD synaptic efficacy corresponding to optimal reward is shifted to a larger value (that is, the decision threshold is lower) when the task is easy, and the opposite is true when the task is hard (Fig. 7c). This result demonstrates that by adjusting the Cx-CD synaptic efficacy, the network is potentially capable of adapting to the statistics of a particular natural sensory environment in order to maximize harvested reward.

DISCUSSION

In this paper we presented a multimodule model for the complete computational process in a reaction time task: integration of information by ramping neural activity in the cortex (Cx), detection of threshold crossing by an all-or-none burst signal in the superior colliculus (SC), and threshold tuning by cortico-striatal synapses in the basal ganglia (BG). In our model, the ramping slope of cortical activity is negatively correlated with the decision time in single trials, consistent with physiological observations^{6,8}. By contrast, the firing threshold does not covary with the decision time, similar to that reported in ref. 8 for neurons of the frontal eye field in a countermanding task. Notably, the decision threshold has a small variability that is the same even as the mean and s.d. of the decision time increase considerably with decreasing coherence. Therefore, the variability of decision time is primarily due to that of ramping slope, as a result of the stochastic spike discharges of cortical neurons.

The biophysically constrained model allows us to investigate cellular and synaptic mechanisms of elemental decision computations. In particular, our results demonstrate a local recurrent circuit mechanism for burst generation in the superior colliculus that serves to detect threshold crossing in the upstream cortical network. High-frequency bursts comparable to those observed in the superior colliculus^{18,36} require relatively long-lasting excitation that may be facilitated by the NMDA receptors, consistent with experimental evidence²³, and on delayed feedback inhibition, which, in our model, depends on the short-term facilitation of excitatory synapses onto GABAergic interneurons. *In vitro* experiments have shown that in the hippocampus and neocortex, certain subtypes of GABAergic interneurons receive excitatory input via unreliable but strongly facilitating synapses^{37,38}. Our model suggests that this would be a desirable feature of feedback inhibition in the superior colliculus as well.

Using the phase plane analysis, we show that in our model there is a dissociation between threshold detection by the superior colliculus and threshold control by the caudate nucleus and the SNr in the basal ganglia. The cortico-striatal connection provides an effective substrate for threshold modulation, because it determines the cortical drive needed to activate the caudate nucleus, thereby suppressing the SNr

and releasing the superior colliculus from inhibition. The key feature here is the steep slope of the SNr trajectory (**Fig. 5a**), which helps the cortico-basal ganglia pathway to gain a dominant role in controlling the decision threshold. This steep slope is consistent with the observation that during behavioral tasks, the firing rate of a subclass of SNr (pausing) neurons drops markedly right before a saccade^{34,35}. As long as the superior colliculus is not disinhibited, it is more difficult to trigger a saccadic eye movement, except for when a powerful, salient stimulus is presented. Hence, the threshold of cortical input to trigger a burst in the superior colliculus is relatively insensitive to the efficacy of cortico-collicular synapses. This is no longer the case when the basal ganglia pathway is disabled (**Supplementary Fig. 1** online). Functional implications of this dissociation can be appreciated by noting that burst neurons in the intermediate layer of the superior colliculus receive a convergence of inputs from many sources, including the LIP, frontal and supplementary eye fields, and primary visual cortex via the superficial layer in the superior colliculus. Without a separate control circuit, burst generation in the superior colliculus, and hence saccadic eye movement, would be susceptible to constant sensory perturbations and small fluctuations in the input. The CD-SNr circuit in the basal ganglia constitutes a mechanism of threshold setting for the superior colliculus, globally for all types of afferent inputs.

Our model is minimal in its architecture and biophysical detail, and can be extended in future studies in several ways. For instance, our model does not include 'fixation neurons' in the superior colliculus^{36,39}, which exhibit a firing pattern similar to that of SNr cells and are believed to inhibit burst cells in the superior colliculus (and could thus provide an additional mechanism for threshold control). Moreover, the inclusion of such fixation neurons could allow our model to simulate the delayed response version of the random-dot discrimination task⁶. The idea is that during a mnemonic delay period interposed between stimulus presentation and saccadic response, the presence of a fixation cue maintains a relatively high activity level in fixation neurons; these cells in turn suppress burst cells in the superior colliculus. Hence, after a decision has been made during stimulation and the choice has been stored in working memory by persistent cortical activity, neurons in the superior colliculus remain inhibited across the delay. At the end of the delay period, the disappearance of the fixation cue leads to a decrease of fixation neural activity; the burst cells are now released from inhibition and generate a burst of spikes signaling the motor response. This scenario deserves to be tested in future studies. We also did not take into account 'buildup/prelude' neurons, which fire sparsely with ramping activity before the saccade onset^{18,36}. Buildup activity has been observed in the superior colliculus during the random-dot direction-discrimination task with a fixed stimulus duration⁴⁰. It remains to be seen whether it occurs in the reaction time version of the task as well and, if so, whether it represents the monkey's motor preparation for an incoming saccade rather than time integration of sensory information.

Moreover, in the present study we did not consider direct inputs from the retina to the superior colliculus (via the superficial layer of the superior colliculus), which (if strong enough) can trigger burst discharges in the intermediate layer of the superior colliculus without disinhibition along the basal ganglia pathway. In a difficult perceptual decision task, such strong inputs are either absent (by experimental design) or present (in more realistic situations), but their effects on burst cells must be suppressed somehow (for example, inhibited by SNr cells or fixation neurons; ref. 39) until sufficient evidence is accumulated and a perceptual judgement is reached. The inner working of such control processes is a topic beyond the scope of the present paper and is worth studying in future work.

Concerning the basal ganglia circuit, striatal output neurons display Up and Down states of membrane potential⁴¹, which were not explicitly incorporated in the simulations reported here. However, our model does assume that striatal cells have a fairly hyperpolarized resting state and require a critical level of cortical excitation to trigger significant spike discharges. Thus the model is consistent with a scenario in which striatal output neurons are endowed with Up and Down membrane potentials and typically reside in the Down state at rest. We did check this possibility by including membrane bistability in CD cells, and we found that the network behavior, as assessed by the psychometric and chronometric functions, was not substantially affected by this single-cell membrane property (**Supplementary Fig. 2** online). It has been proposed that membrane bistability of striatal cells is modulated by dopamine⁴², and its effects on signal processing (and on threshold tuning in particular) remain to be assessed. Furthermore, in addition to the direct CD-SNr pathway, the striatum also sends its output through an 'indirect' pathway that extends from the CD to the external segment of the globus pallidus and thence to the subthalamic nucleus and the SNr (refs. 25,28). The indirect pathway is likely to produce global inhibition of undesired saccades^{43,44}, but it is unknown and deserves to be examined whether, in interplay with the direct pathway, the indirect pathway also has a role in the modulation of a decision threshold.

It has been suggested that the rate of reward harvest can be tuned by varying a decision threshold^{11,15}, but how this may be accomplished in the brain remains an open question. Our results identify a specific anatomical substrate at the cortico-striatal (Cx-CD) synapses. Strong cortico-striatal efficacy produces a low decision threshold, which generates quick responses but poor performance, whereas weak cortico-striatal efficacy yields a high decision threshold, which generates slow responses but better performance. Our model predicts that the firing rate of cortical decision neurons at the onset of the saccade should vary adaptively in behavioral tasks that require a trade-off between speed and accuracy, a prediction that can be tested experimentally. In a human behavioral study using the random-dot discrimination task¹⁶, subjects were instructed to aim at producing a mean reaction time of 0.5 s, 1 s or 2 s. Using the bounded diffusion model to fit the behavioral data, the authors found that the bound height, as well as the average speed and accuracy, changed when the subjects were instructed to respond with different speeds. Note that the instruction provided additional information that the subject may have used, such as an estimate of interval timing (0.5 s, 1 s or 2 s), that our model does not incorporate. Nevertheless, we found that our model could reproduce the observations for the speed instructions of 0.5 s and 1.0 s: the behavioral performance and reaction time corresponded to those predicted by our model for cortico-striatal efficacies of 3.8 nS and 0.8 nS, respectively (**Supplementary Fig. 3** online).

Our model suggests that as a result of the speed-accuracy trade-off, the reward rate shows an inverted-U-shaped dependence on cortico-striatal synaptic efficacy: a maximum reward rate occurs at an intermediate cortico-striatal efficacy. Furthermore, our model shows that the optimal cortico-striatal efficacy, or threshold, is adjustable when the statistics of sensory stimuli in the environment change, a prediction that can be tested readily in laboratory experiments. Although the amount of change in the reward rate across different Cx-CD efficacies looks small (**Fig. 7a**), the effect can be increased by using narrower distributions of coherence levels (**Fig. 7c**). One might argue that animals can only sense a rough change in the reward rate and thus can only tune the Cx-CD efficacy to within an approximate range around the optimal value, not to the exact optimal value. Nevertheless, our model predictions can be tested by using distinct

coherence levels, say, 2–10% in one session of trials and 40–50% in another session.

Our finding of tunable threshold through cortico-striatal synapses is notable especially in light of the fact that modification of cortico-striatal connections is strongly modulated by reward signals mediated by the dopamine system^{31,32}. Therefore, a mechanism for tunable threshold can be implemented by the cortico-striatal synaptic plasticity that follows a reward-dependent Hebbian-like learning rule⁴⁵. More specifically, the activated cortico-striatal synapses increase their strength by a small amount in rewarded trials and reduce it in error trials. Such cortico-striatal synaptic modifications in turn alter choice behavior and thus the reward rate itself. It will be worth investigating, within this framework, the optimal reward behavior in terms of learning induced by the dynamical interaction in the reciprocal loop between the cortico-basal ganglia system and the dopaminergic reward system^{26–28}. Moreover, our model endowed with synaptic plasticity would also lead to threshold modulation across many trials, thereby providing an explanation of reward-dependent choice bias over long timescales^{29,46}.

In summary, we have presented a biophysically based network model that can completely simulate a reaction time task, from the integration of sensory inputs to threshold detection and tuning. Our model suggests a parallel circuit mechanism, in which the decision threshold is detected along the cortico-collicular pathway and tuned through the cortico-basal ganglia pathway. Our results indicate that the regulation of decision threshold represents a specific computational mechanism through which cortico-striatal synaptic plasticity can contribute to adaptive behavior and to sensorimotor learning in general²⁷.

METHODS

Behavioral task. Our model aims to simulate the random-dot direction-discrimination task^{3,6}. To be concrete, we assume the direction of coherent motion to be either rightward or leftward. In our model, two inputs (presumably from area MT; ref. 47) representing the rightward and leftward moving dots are fed into Cx^R and Cx^L , respectively, in the cortical network (Fig. 1). The firing rate of each input neuron follows a Poisson rate that varies in time with a Gaussian distribution of mean μ . The mean μ depends on the coherence level linearly and follows the equations $\mu = \mu_0 + \mu_A \times c'$ for the preferred direction and $\mu = \mu_0 - \mu_B \times c'$ for the nonpreferred direction, where μ_0 (20 Hz) is the baseline input, c' (between 0% and 100%) is the coherence level, and μ_A (60 Hz) and μ_B (20 Hz) are factors of proportionality. We assume a synaptic conductance $g = 4.2$ nS, which represents the product of the number of MT input connections onto a cortical neuron and the conductance of individual MT-Cxe synapses. Ref. 47 reported that the population average of the slopes of MT neuron firing rates as a function of coherence is 3.5 times higher in the preferred direction than in the nonpreferred direction⁴⁷ (or $\mu_A \sim 3.5\mu_B$). Given the fact that μ_A and μ_B for individual MT neurons follow broad distributions⁴⁷, our assumption of $\mu_A = 3\mu_B$ is not substantially different from these observations⁴⁷. The decision time is defined as the time interval between the start of the sensory input to Cx and the onset of SCe burst activity. The response time is the decision time plus a 250-ms-long non-decision time (such as visual latency and motor response time). A correct trial is defined as a trial in which the model generates a saccadic burst in the same direction as the coherent motion.

Large-scale circuit model. Our model includes a cortical network, a superior colliculus network and a basal ganglia network (Fig. 1). Single neurons are generally modeled by the leaky integrate-and-fire model, and synaptic currents are described by realistic gating kinetics (details in **Supplementary Methods** online).

The cortical network (Cx) model was adopted from ref. 13. The model contains two populations (Cx^R and Cx^L) with recurrent excitation. Each population contains 240 excitatory neurons and responds to random-dot motion in one of two opposite directions. The populations compete with each

other through an inhibitory population (Cxi) of GABAergic neurons. The system exhibits winner-take-all competition: the excitatory population, which receives a stronger input, has a greater chance of building up its firing rate and winning the competition. This behavior resembles that observed in the LIP in the random-dot experiment⁶. In the present study, we did not use a preset threshold as in ref. 13. Instead, the cortical network projects to downstream neurons in the superior colliculus and the basal ganglia.

In the superior colliculus (SC) model, we address the burst-generating mechanism and the nonlinear response of neurons in the superior colliculus to external stimuli²³. Local excitatory and inhibitory circuits in the superior colliculus are known to be essential for burst generation^{21–24}. Experimental studies have shown that burst firing of neurons in the superior colliculus depends on NMDA receptors²³. On the other hand, GABAergic neurons are widely distributed throughout the superior colliculus⁴⁸ and presumably underlie the observed lateral inhibition in behaving animals³⁹. Based on these experimental observations, we constructed a three-population model for burst generation in the superior colliculus (Fig. 1): two populations of 250 excitatory neurons (SCe^R and SCe^L) with recurrent excitation through NMDA receptors and one population of 250 inhibitory neurons (SCi). Each of SCe^R and SCe^L is selective for one of the two direction choices^{18–20,39} and receives inputs from the corresponding cortical neural population (Cx^R or Cx^L). The SCi neurons receive inputs from both SCe populations through NMDA receptors and send inhibitory feedback to both of them through GABA_A receptors³⁹. We further assume that SCe^R -to-SCi and SCe^L -to-SCi synapses exhibit short-term facilitation. For the sake of simplicity, we did not explicitly model projections from SC to the thalamus and back to the cortex⁴⁹. However, we assume that both SCe^R and SCe^L send feedback to all populations in the Cx network to inform the cortex about the execution of a saccade, and resets the Cx network.

In the basal ganglia (BG) model, we focus on how the basal ganglia modulates the timing and the performance of decision making. We modeled the cortico-basal ganglia-superior collicular pathway with two nuclei, CD and SNr. Each nucleus consists of two populations selective for two alternative directions of decision choice. Each population contains 250 GABAergic neurons. CD neurons receive excitatory inputs from Cx through AMPA receptors and exert inhibition on SNr through GABA_A receptors. SNr neurons exhibit tonic baseline activity with a firing rate around 80 Hz and exert inhibition on SCe neurons through GABA_A receptors. We note that anatomically it is still not established whether ramping neurons in cortical networks participate in the cortico-striatal projection. Moreover, physiologically, striatal neurons in the caudate nucleus are heterogeneous and have been found to exhibit movement-, vision- and/or memory-related activities. Nevertheless, some neurons in the caudate nucleus have been reported to display ramping activity during delay periods in certain saccade tasks⁵⁰. Therefore, in addition to traditionally suggested movement neurons, it is likely that the caudate nucleus also receives inputs from other types of neurons (including ramping neurons) in upstream cortical networks.

Details of the model and parameter values for the connections within and between each of three networks are given in **Supplementary Methods**.

Phase plane. The state boundary in the phase plane (Fig. 5a) is constructed by the following procedure. We remove CD from the network and hold the SNr firing rate at a given value. Then we slowly increase Cx firing rate from 0 Hz until it reaches a critical value that generates a burst in SCe. We run 200 trials and calculate the mean critical value of Cx firing rate, which represents one point on the state boundary at the given SNr firing rate. We plot the entire boundary by repeating this procedure with different SNr firing rates. The system trajectory is produced by removing SC from the network and slowly increasing Cx firing rate from 0 Hz until SNr firing rate drops to 0 Hz. The system trajectory is plotted using the SNr response as a function of Cx firing rate averaged over 200 trials.

Reward rate. The reward rate R is defined by $R = P/T$, where P is the performance and T the average trial time duration¹¹. The performance P , defined as the percentage of correct decision choice in a block of trials, is given by $P = \sum_{i=1}^N n_i p_i$, where i denotes the index for the coherence level, n_i is the percentage of trials with the coherence level i , and p_i is the probability of

making a correct choice. The average trial time T is calculated as

$$T = \sum_{i=1}^N n_i [p_i(t_i + t_L + t_{ITI}) + (1 - p_i)(t'_i + t_L + t_{ITI} + t_{penalty})]$$

where t_i is the average decision time of correct trials, t'_i is the average decision time of error trials, t_L is the non-decision time (assumed to be 250 ms), t_{ITI} (0.5 s) is the intertrial interval, and $t_{penalty}$ (2.5 s) is the penalty time added after an error trial. In the simulation, we used six coherence levels, $i = 1-6$, with coherence of 0%, 3.2%, 6.4%, 12.8%, 25.6% and 51.2%, respectively. In **Figure 7a**, each point was calculated using equal probability for all six coherence levels ($n_i = 1/6$ for all i). In **Figure 7b,c**, $\{n_i\} = \{0, 1/3, 1/3, 1/3, 0, 0\}$ for the more difficult task (red curves) and $\{n_i\} = \{0, 0, 0, 1/3, 1/3, 1/3\}$ for the easier task (black curves). For each value of Cx-CD efficacy, t_i and p_i were calculated based on N_i number of trials, where $\{N_i\} = \{1,200, 2,400, 1,800, 1,800, 600, 600\}$. We used a larger number of trials in the cases of lower coherence levels due to the larger variation in t_i and p_i .

Note: Supplementary information is available on the Nature Neuroscience website.

ACKNOWLEDGMENTS

We thank S. Fusi for early work on the computer program used in this study, and D. Lee and P. Miller for helpful comments on the manuscript. This work was supported by the Swartz Foundation and the US National Institutes of Health (MH 062349).

COMPETING INTERESTS STATEMENT

The authors declare that they have no competing financial interests.

Published online at <http://www.nature.com/natureneuroscience>

Reprints and permissions information is available online at <http://npg.nature.com/reprintsandpermissions/>

- Luce, R.D. *Response Times* (Oxford University Press, New York, 1986).
- Usher, M. & McClelland, J.L. The time course of perceptual choice: the leaky, competing accumulator model. *Psychol. Rev.* **108**, 550–592 (2001).
- Reddi, B.A.J., Asrress, K.N. & Carpenter, R.H.S. Accuracy, information, and response time in a saccadic decision task. *J. Neurophysiol.* **90**, 3538–3546 (2003).
- Ratcliff, R. & Smith, P.L. A comparison of sequential sampling models for two-choice reaction time. *Psychol. Rev.* **111**, 333–367 (2004).
- Newsome, W.T., Britten, K.H. & Movshon, J.A. Neuronal correlates of a perceptual decision. *Nature* **341**, 52–54 (1989).
- Roitman, J.D. & Shadlen, M.N. Response of neurons in the lateral intraparietal area during a combined visual discrimination reaction time task. *J. Neurosci.* **22**, 9475–9489 (2002).
- Kim, J.N. & Shadlen, M.N. Neural correlates of a decision in the dorsolateral prefrontal cortex of the macaque. *Nat. Neurosci.* **2**, 176–185 (1999).
- Hanes, D.P. & Schall, J.D. Neural control of voluntary movement initiation. *Science* **274**, 427–430 (1996).
- Schall, J.D. & Thompson, K.G. Neural selection and control of visually guided eye movements. *Annu. Rev. Neurosci.* **22**, 241–259 (1999).
- Gold, J.I. & Shadlen, M.N. Neural computations that underlie decisions about sensory stimuli. *Trends Cogn. Sci.* **5**, 10–16 (2001).
- Gold, J.I. & Shadlen, M.N. Banburismus and the brain: decoding the relationship between sensory stimuli, decisions, and reward. *Neuron* **36**, 299–308 (2002).
- Smith, P.L. & Ratcliff, R. Psychology and neurobiology of simple decisions. *Trends Neurosci.* **27**, 161–168 (2004).
- Wang, X.-J. Probabilistic decision making by slow reverberation in cortical circuits. *Neuron* **36**, 955–968 (2002).
- Wong, K.-F. & Wang, X.-J. A recurrent network mechanism of time integration in perceptual decisions. *J. Neurosci.* **26**, 1314–1328 (2006).
- Brown, E. *et al.* Simple neural networks that optimize decisions. *Int. J. Bifurc. Chaos* **15**, 803–826 (2005).
- Palmer, J., Huk, A.C. & Shadlen, M.H. The effect of stimulus strength on the speed and accuracy of a perceptual decision. *J. Vis.* **5**, 376–404 (2005).
- Hall, W.C., Moschovakis, A. (eds.). *The Superior Colliculus: New Approaches for Studying Sensorimotor Integration* (CRC Press, New York, 2003).
- Munoz, D.P. & Wurtz, R.H. Saccade-related activity in monkey superior colliculus. I. Characteristics of burst and buildup cells. *J. Neurophysiol.* **73**, 2313–2333 (1995).
- Sparks, D.L. The brainstem control of saccadic eye movements. *Nat. Rev. Neurosci.* **3**, 952–964 (2002).
- Scudder, C.A., Kaneko, C.R.S. & Fuchs, A.F. The brainstem burst generator for saccadic eye movements: a modern synthesis. *Exp. Brain Res.* **142**, 439–462 (2002).
- Pettit, D.L., Helms, M.C., Lee, P.L., Augustine, G.J. & Hall, W.C. Local excitatory circuits in the intermediate gray layer of the superior colliculus. *J. Neurophysiol.* **81**, 1424–1427 (1999).
- Saito, Y. & Isa, T. Electrophysiological and morphological properties of neurons in the rat superior colliculus. I. Neurons in the intermediate layer. *J. Neurophysiol.* **82**, 754–767 (1999).
- Saito, Y. & Isa, T. Local excitatory network and NMDA receptor activation generate a synchronous and bursting command from the superior colliculus. *J. Neurosci.* **23**, 5854–5864 (2003).
- Saito, Y. & Isa, T. Laminar specific distribution of lateral excitatory connections in the rat superior colliculus. *J. Neurophysiol.* **92**, 3500–3510 (2004).
- Hikosaka, O., Takikawa, Y. & Kawagoe, R. Role of the basal ganglia in the control of purposive saccadic eye movements. *Physiol. Rev.* **80**, 953–978 (2000).
- Houk, J.C., Davis, J.L. & Beiser, D.G. (eds.). *Model of Information Processing in the Basal Ganglia* 2nd edn. (MIT Press, Cambridge, Massachusetts, 1998).
- Graybiel, A.M. Building action repertoires: memory and learning functions of the basal ganglia. *Curr. Opin. Neurobiol.* **5**, 733–741 (1995).
- Wickens, J. Basal ganglia: structure and computations. *Network: Comput. Neural Syst.* **8**, 77–109 (1997).
- Hikosaka, O., Nakamura, K. & Nakahara, H. Basal ganglia orient eyes to reward. *J. Neurophysiol.* **95**, 567–584 (2006).
- Nicola, S.M., Surmeier, D.T. & Malenka, R.C. Dopaminergic modulation of neuronal excitability in the striatum and nucleus accumbens. *Annu. Rev. Neurosci.* **23**, 185–215 (2000).
- Reynolds, J.N.J., Hyland, B.I. & Wickens, J.R. A cellular mechanism of reward-related learning. *Nature* **413**, 67–70 (2001).
- Schultz, W. Getting formal with dopamine and reward. *Neuron* **36**, 241–263 (2002).
- Kawagoe, R., Takikawa, Y. & Hikosaka, O. Reward-predicting activity of dopamine and caudate neurons—a possible mechanism of motivational control of saccadic eye movement. *J. Neurophysiol.* **91**, 1013–1024 (2004).
- Hikosaka, O. & Wurtz, R.H. Visual and oculomotor functions of monkey substantia nigra pars reticulata. I. Relation of visual and auditory responses to saccades. *J. Neurophysiol.* **49**, 1230–1253 (1983).
- Saito, M. & Hikosaka, O. Role of primate substantia nigra pars reticulata in reward-oriented saccadic eye movement. *J. Neurosci.* **22**, 2363–2373 (2002).
- Munoz, D.P., Dorris, M.C., Pare, M. & Everling, S. On your mark, get set: brainstem circuitry underlying saccadic initiation. *Can. J. Physiol. Pharmacol.* **78**, 934–944 (2000).
- Ali, A.B. & Thomson, A.M. Facilitating pyramid to horizontal oriens-alveus interneurone inputs: dual intracellular recordings in slices of rat hippocampus. *J. Physiol. (Lond.)* **507**, 185–199 (1998).
- Markram, H., Wang, Y. & Tsodyks, Y. Differential signaling via the same axon of neocortical pyramidal neurons. *Proc. Natl. Acad. Sci. USA.* **95**, 5323–5328 (1998).
- Munoz, D.P. & Istvan, P.J. Lateral inhibitory interactions in the intermediate layers of the monkey superior colliculus. *J. Neurophysiol.* **79**, 1193–1209 (1998).
- Horwitz, G.D. & Newsome, W.T. Target selection for saccadic eye movements: prelude activity in the superior colliculus during a direction-discrimination task. *J. Neurophysiol.* **86**, 2543–2558 (2001).
- Wilson, C.J. & Kawaguchi, Y. The origins of two-state spontaneous membrane potential fluctuations of neostriatal spiny neurons. *J. Neurosci.* **16**, 2397–2410 (1996).
- Gruber, A.J., Solla, S.A., Surmeier, D.J. & Houk, J.C. Modulation of striatal single units by expected reward: a spiny neuron model displaying dopamine-induced bistability. *J. Neurophysiol.* **90**, 1095–1114 (2003).
- Jiang, H., Stein, B.E. & McHaffie, J.G. Opposing basal ganglia processes shape midbrain visuomotor activity bilaterally. *Nature* **423**, 982–986 (2003).
- Frank, M.J., Seeberger, L.C. & O'Reilly, R.C. By carrot or by stick: cognitive reinforcement learning in parkinsonism. *Science* **306**, 1940–1943 (2004).
- Soltani, A. & Wang, X.-J.A. Biophysically based neural model of matching law behavior: melioration by stochastic synapses. *J. Neurosci.* **26**, 3731–3744 (2006).
- Lauwereyns, J., Watanabe, K., Coe, B. & Hikosaka, O. A neural correlate of response bias in monkey caudate nucleus. *Nature* **418**, 413–417 (2002).
- Britten, K.H., Shadlen, M.N., Newsome, W.T. & Movshon, J.A. Responses of neurons in macaque MT to stochastic motion signals. *Vis. Neurosci.* **10**, 1157–1169 (1993).
- Behan, M., Steinhacker, K., Jeffrey-Borger, S. & Meredith, M.A. Chemoarchitecture of GABAergic neurons in the ferret superior colliculus. *J. Comp. Neurol.* **452**, 334–359 (2002).
- Sommer, M.A. & Wurtz, R.H. What the brain stem tells the frontal cortex. II. Role of the SC-MD-FF pathway in corollary discharge. *J. Neurophysiol.* **91**, 1403–1423 (2004).
- Hikosaka, O., Sakamoto, M. & Usui, S. Functional properties of monkey caudate neurons. I. Activities related to saccadic eye movements. *J. Neurophysiol.* **61**, 780–798 (1989).

